Published in final edited form as:

Nature. 2009 August 20; 460(7258): 984–989. doi:10.1038/nature08217.

Specific pathways prevent duplication-mediated genome rearrangements

Christopher D. Putnam, **Tikvah K. Hayes**, and **Richard D. Kolodner**

Ludwig Institute for Cancer Research, Departments of Medicine and Cellular and Molecular Medicine and Cancer Center, University of California School of Medicine, San Diego, 9500 Gilman Drive, La Jolla, CA 92093-0669

SUMMARY

We have investigated the ability of different regions of the left arm of *Saccharomyces cerevisiae* chromosome V to participate in the formation of gross chromosomal rearrangements (GCRs). We found that the 4.2 kb *HXT13 DSF1* region sharing divergent homology with chromosomes IV, X, and XIV, similar to mammalian segmental duplications, was “at-risk” for participating in duplication-mediated GCRs generated by homologous recombination. Numerous genes and pathways, including SGS1, TOP3, RMI1, SRS2, RAD6, SLX1, SLX4, SLX5, MSH2, MSH6, *RAD10* and the DNA replication stress checkpoint requiring *MRC1* and *TOF1* were highly specific for suppressing these GCRs compared to GCRs mediated by single copy sequences. These results indicate that the mechanisms for formation and suppression of rearrangements occurring in regions containing “at risk” sequences differ from those occurring in regions of single copy sequence. This explains how extensive genome instability is prevented in eukaryotic cells whose genomes contain numerous divergent repeated sequences.

INTRODUCTION

The importance of maintaining the stability of the genome is revealed by the numerous genetic diseases caused by inherited and *de novo* mutations ranging from base changes to genome rearrangements1, 2. In addition, many cancers are associated with ongoing genome instability and the continued accumulation of mutations and genome rearrangements3-7. Despite the problems introduced by genome instability, the human genome contains many features prone to be unstable, including microsatellite repeats, minisatellite repeats, triplet repeats, short separated repeats, mirror repeats, inverted repeats, and dispersed repetitive elements such as retroviral elements, SINEs, LINEs, segmental duplications and regions of

Address correspondence to: Richard D. Kolodner Ludwig Institute for Cancer Research 9500 Gilman Drive La Jolla, CA 92093-0669 rkolodner@ucsd.edu (858) 534-7804 (phone) (858) 822-4479 (fax). Correspondence and requests for materials should be addressed to rkolodner@ucsd.edu..

AUTHOR CONTRIBUTIONS C.D.P., R.D.K. and T.K.H. designed the experiments. C.D.P. and T.K.H. performed the experiment. C.D.P. and R.D.K. analyzed the data and wrote the manuscript.

AUTHOR INFORMATION Microarray data has been submitted to ArrayExpress (ebi.ac.uk/arrayexpress) with accession number E-TABM-714. Reprints and permissions information is available at npg.nature.com/reprintsandpermissions.

The authors declare no competing financial interests.

copy number variation (CNVs)8, 9. Dispersed repetitive elements can underlie chromosomal rearrangements through non-allelic homologous recombination (HR) between elements at non-homologous chromosomal locations. The Alu elements, for example, cause HR-mediated deletions, duplications, and chromosomal translocations implicated in over 15 inherited diseases as well as rearrangements leading to cancer10. Similarly, more than 20 human diseases are caused by rearrangements mediated by non-allelic HR between segmental duplications11. Given the large numbers of repeated regions in the genome, it is surprising that the genome is as stable as it is.

Some types of "at-risk" sequences have been characterized in *Saccharomyces cerevisiae*9. Engineered duplications are targets of ectopic recombination, leading to both gene conversion and chromosomal rearrangements12. Similarly, Ty transposons, which are dispersed, repeated sequences, can recombine to produce genome rearrangements13, and inverted copies of Ty transposons can cause DSBs during replication resulting in genome rearrangements14. Consistent with this, "at-risk" sequences appear to be selected against15; however, the human genome still retains many such sequences. While "at-risk" sequences can induce genome instability, little is known about how such genome rearrangements are prevented and whether there are specific pathways that prevent such sequences from causing genome rearrangements.

We have described assays for measuring the rate of accumulating gross chromosomal rearrangements (GCRs)16. This assay system detects GCRs that occur in natural DNA sequences and does not depend on the introduction of artificial DNA sequences or the artificial induction of DSBs. Here, we applied this system to compare the rates and properties of GCRs in a chromosomal region devoid of "at-risk" sequences with that of a region of the genome containing a sequence homeologous to ectopic regions of the the genome reminiscent of segmental duplications.

RESULTS

Duplications alter the GCR spectrum and rate

We placed a *CAN1/URA3* cassette in different locations on the non-essential left end of chromosome V to select for canavanine (Can) and 5-fluoroorotate (5FOA) resistant GCRs similar to our original GCR assay16 (Fig. 1A). GCRs, but not co-mutation or interstitial co-deletion of *CAN1* and *URA3*, dominated the Can^r $5FOA^r$ products as evidenced by frequent loss of a telomeric hygromycin-resistance marker (Suppl. Table 1), similar to the original GCR assay17. Overall, the GCR rates increased approximately linearly with the size of the chromosome V breakpoint region except for the *yel072w::CAN1/URA3* assay, which had a higher rate than predicted based on the breakpoint region length (Table 1). *YEL072W* is telomeric to the *HXT13 DSF1* region, which shares ~4.2 kb of imperfect homology with chromosome XIV and ~2 kb of imperfect homology with nearly identical regions of chromosomes IV and X (Fig. 1B), similar to mammalian segmental duplications18. Deletion of *HXT13 DSF1* eliminated the duplication-associated GCR rate increase (Table 1). Homology-driven monocentric t(V;XIV) and t(V;IV or X) translocations accounted for 90% of the GCRs even though the *HXT13 DSF1* region accounts for 13% of the breakpoint region (Fig. 2A). Sequencing of 20 t(V;XIV) junctions only revealed translocation

breakpoints in the *HXT13 DSF1* homology regions (Suppl. Fig. 1A)17. Array comparative genomic hybridization (aCGH) demonstrated that the target chromosomes were duplicated from the homology to the telomere (Fig. 1C), indicating that an intact copy of the target chromosomes were maintained; this was confirmed by PCR amplification of the native *HXT13 DSF1* related junctions on the target chromosome (data not shown). Overall, the homology-driven GCRs were consistent with break-induced replication (BIR) or related mechanisms19, 20.

Genotype affects the impact of the duplication

In the standard GCR assay, deletion of *MRE11* or *RAD27* caused ~600-1000 fold increased GCR rates16 and caused similar rate increases in strains where the *CAN1/URA3* cassette was centromeric to *HXT13 DSF1* (Table 1). When the cassette was telomeric to the duplication, the mutations only caused a modest increase in GCR rate relative to the *yel068c::CAN1/URA3* assay: five-fold for *rad27*Δ and three-fold for *mre11*Δ. The GCRs in the *rad27*Δ *yel072w::CAN1/URA3* background were a mix of 33 duplication-mediated and 16 single-copy sequence-mediated products (Fig. 2A). Like the wild-type strain that had 56 duplication-mediated and 6 single-copy sequence-mediated GCRs, the ratios of products were similar to the fold increase in rate caused by the duplication. In contrast, the *mre11*Δ *yel072w::CAN1/URA3* GCRs were dominated by duplication-mediated rearrangements (56:1). This suggests that an *mre11*Δ mutation alters the mechanism underlying GCRs such as by decreasing telomere maintenance21 resulting in increased degradation of chromosome ends, which would preferentially target telomeric duplicated sequences.

Deletion of *SGS1*, encoding a RecQ-family helicase, caused a moderate increase in the rate of GCRs in assays with the *CAN1/URA3* cassette centromeric to the duplication similar to the standard GCR assay, but caused a dramatic increase in the *yel072w::CAN1/URA3* GCR rate that depended on the *HXT13 DSF1* duplication (Table 1). The ratio of duplication-mediated to single copy sequence-mediated GCRs in the *sgs1*Δ mutant, 35:5 (Fig. 2A), was not as high as might be predicted from the 115-fold increase in GCR rates in the *yel072w::CAN1/URA3* assay vs. the *yel068c::CAN1/URA3* assay. Sequencing of 25 *sgs1*Δ t(V;XIV) breakpoint junctions revealed 21 t(V;XIV) and 4 complex translocations (Suppl. Fig. 1B). Three complex breakpoints resulted from t(V;XIV;V;XIV) translocations, and the fourth was consistent with a t(V;X;XIV) translocation. The complex junctions could be generated by template-switching during HR as implicated during BIR in wild-type strains22 and *CAN1-LYP1-ALP1* translocations in *sgs1*Δ mutants23, or by formation of multiduplex joint molecules as observed in meiosis24.

Different HR pathways yield distinct GCR signatures

We next examined the role of the *RAD52* epsistasis group genes (Table 2). As in the standard GCR assay25, the *rad52*Δ mutation increased the GCR rate in the *yel068c::CAN1/URA3* assay where GCRs are formed in single copy DNA sequences (Table 2). In contrast, the *rad52*Δ mutation modestly decreased the GCR rate in the *yel072w::CAN1/URA3* assay compared to wild-type (Table 2) and eliminated the duplication-mediated translocations (Fig. 2B). Deletion of *RAD51* or *RAD59*, which define two distinct *RAD52*-dependent HR pathways26, had modest effects on the GCR rates in both assays, and non-reciprocal

duplication-mediated translocations were observed in both single mutants (Table 2; Fig. 2B; Suppl. Fig. 2), indicating that these rearrangements are not strictly dependent on either pathway. t(V;IV or X) translocations were not observed in the *rad59*Δ strain, suggesting that efficient recombination with the translocation target that was shorter and had lower sequence identity was *RAD59* dependent. Both the *rad51*Δ *rad59*Δ double mutant and the *rad51*Δ *rad59*Δ *rad52*Δ triple mutant had decreased rates of duplication-mediated GCRs (Table 2). Surprisingly, t(V;XIV) rearrangements were observed in the *rad51*Δ *rad59*Δ double mutant, unlike the *rad52*Δ single mutant and the *rad51*Δ *rad59*Δ *rad52*Δ triple mutant (Fig. 2B). Thus, it appears that at least one additional *RAD52*-dependent, *RAD51*- and *RAD59*- independent HR pathway can promote interchromosomal HR-mediated rearrangements at low rates; this is consistent with a more severe HR defect in a *rad52*Δ single mutant compared to a *rad51*Δ *rad59*Δ double mutant27.

Mismatch repair (MMR) proteins28 and Sgs129 are predicted to suppress HR between the *HXT13 DSF1* region and the imperfect homologies on chromosomes IV, X, and XIV. Elimination of mismatch detection by a *msh2*Δ mutation or impairment by *msh6*Δ or *msh3*Δ mutations specifically increased the GCR rates in the duplication-containing assay (Table 2). The larger effects of *msh2*Δ and *msh6*Δ relative to *msh3*Δ are consistent with the heteroduplexes formed during duplication-mediated HR, which would contain primarily base-base mispairs and fewer insertion/deletion mispairs. Similar to the effects of *mlh1*Δ in single-stranded annealing assays30, *mlh1*Δ caused a smaller but significant increase in the rate of duplication-mediated GCRs (Table 2). An *sgs1*Δ mutation caused an increase in duplication-mediated GCRs (Table 1 and Fig. 2), and a *rad52*Δ mutation eliminated this increase (Table 2), indicating that homeologous recombination mediates most of the GCRs in the *yel072*::*CAN1/URA3* assay in the *sgs1*Δ mutant. However, *sgs1*Δ caused a higher duplication-mediated GCR rate than *msh2*Δ (Table 2), despite the fact that Sgs1 is downstream of MMR during suppression of homeologous recombination30. Deletion of *TOP3* and *RMI1*, which function in concert with *SGS1*31, also caused higher rates of duplication-mediated GCRs than the *msh2*Δ mutation; the increased GCR rates caused by *rmi1*Δ relative to *sgs1*Δ and *top3*Δ suggests that *RMI1* may have *SGS1*- and *TOP3*-independent roles (Table 2). These data, in combination with the synergistic increase in the GCR rate in the *yel068c*::*CAN1/URA3* assay in the *sgs1*Δ *rad52*Δ double mutant (Table 2) suggests that *sgs1*Δ as well as *top3*Δ and *rmi1*Δ cause defects in suppression of homeologous recombination and also affect other pathways that suppress duplication-mediated GCRs.

HR-mediated GCRs are *POL32*-independent

The t(V;XIV) and t(V;IV or X) translocation products and their dependence on HR genes are consistent with BIR or related mechanisms19, 20. *POL32*, encoding a DNA polymerase delta subunit, is essential for ectopic BIR induced by HO-mediated DSBs32, but not strictly required for allelic BIR20. Deletion of *POL32* caused a small increase in the duplication-mediated GCR rate and did not change the rate of t(V;XIV) or t(V;IV or X) translocations (Table 2; Fig. 2B). The three *pol32*Δ t(V;XIV) translocations analyzed by aCGH were non-reciprocal (Suppl. Fig. 3). These results could be explained if previously observed *POL32*-

dependent BIR was predominantly *RAD51*-dependent32, in contrast to both *RAD51*-dependent and *RAD51*-independent pathways observed here.

Both the *pol32*Δ *rad51*Δ and *pol32*Δ *rad59*Δ double mutants had low levels of duplication-mediated GCRs (Table 2, Fig. 2B). The *pol32*Δ *rad51*Δ double mutant had increased GCR rates in both assays, with the duplication causing a modest increase primarily due to accumulation of t(V;IV or X) translocations, consistent with the possibility that *RAD51* is required to suppress GCRs in a *pol32*Δ mutant. In contrast, the *pol32*Δ *rad59*Δ double mutant had a lower GCR rate than the *rad59*Δ and *pol32*Δ single mutants, and, compared to the *rad51*Δ *rad59*Δ double mutant, had a similar GCR rate in the *yel072w::CAN1/URA3* assay and a somewhat lower rate in the *yel068c::CAN1/URA3* assay. In addition, the rate of t(V;XIV) translocations was reduced in the *pol32*Δ *rad59*Δ mutant relative to *pol32*Δ and *rad59*Δ single mutants, but not to the extent seen in *rad51*Δ *rad59*Δ double mutants (Fig. 2B). These results suggest that *POL32* functions in the *RAD51*-dependent pathway but not the *RAD59*-dependent pathway that promotes duplication-mediated GCRs; however, in the *RAD51*-dependent pathway, the formation of duplication-mediated GCRs is not completely dependent on *POL32*. Thus, a subset of the *RAD51*-dependent duplication-mediated GCRs are likely produced by *POL32*-dependent BIR, whereas *POL32*-independent *RAD51*-dependent and *RAD59*-dependent duplication-mediated GCRs either result from other HR mechanisms, such as a half-crossover mechanism20, or are produced by a BIR pathway that has different genetic requirements than BIR driven by HO-induced DSBs. Two other replication-associated mutations, *pri2-1*, which suppresses HR-mediated BIR32, and *pol12-100*, which increases levels of Holliday junctions during replication33, generally decreased or weakly increased GCR rates, respectively.

Pathways that suppress HR-mediated GCRs

As analysis of *sgs1*Δ, *top3*Δ, *rmi1*Δ, *msh2*Δ and *msh6*Δ mutants (Table 2) indicated that the *yel072w::CAN1/URA3* assay can reveal pathways that specifically suppress duplication-mediated rearrangements, we screened for additional context-specific mutations (Table 3). Deletion of *SGS1* causes synthetic growth defects with deletions of *SLX1, SLX4, SLX5, SLX8, MUS81, SAE2, SRS2* or *RRM3*. Deletion of each of these genes, except *SAE2*, caused duplication specific increases in GCR rates whereas only deletion of *SAE2* and *MUS81* caused increases in GCRs mediated by single copy DNA sequences. Similarly, deletion of the repair genes *RAD6, MPH1, RAD10* or *EXO1* caused large increases in duplication-specific GCR rates, but little or no increase in single-copy sequence mediated GCRs. The duplication-specific effects of *rad10*Δ contrast with prior findings that the Rad1-Rad10 complex is required for single-copy DNA sequence mediated GCRs34. Deletion of *ESC2* and *ESC4*/*RTT107*, which encodes a protein recruited to stalled replication forks38, caused a general increase in GCR rates and a preferential increase in the rate of *HXT13 DSF1* duplication-mediated GCRs. Defects in chromatin modifying pathways caused by deletion of *ASF1, RTT109, ARP8* or *NHP10* also had duplication-specific effects; however, in contrast to deleting *ASF1* or *RTT109*, deleting *ARP8* and *NHP10*, which encode subunits of the Ino80 chromatin remodeling complex35, did not alter the rate of single-copy sequence mediated GCRs. In contrast, deletion of *CTF18*, which causes sister chromatid cohesion defects36, caused similar increases in both assays. These results demonstrate that the

genetics of suppressing GCRs changes substantially depending on chromosomal features in the breakpoint region.

Checkpoint suppression of HR-mediated GCRs

Deletion of *MRC1*, which encodes a Rad53 coactivator with roles in DNA replication and replication stress checkpoint signaling37, caused a small increase in the rate of single copy sequence mediated GCRs and a large increase in *HXT13 DSF1* duplication-mediated GCRs. The latter GCRs were primarily homology-driven translocations (Fig. 2A) and 2 GCRs predicted to be t(V;XIV) translocations by PCR were non-reciprocal translocations (Suppl. Fig. 3) similar to all other duplication-mediated GCRs analyzed by aCGH (Fig. 1C, Suppl. Fig. 2 & 3). The *mrc1-aq* allele, which specifically affects the checkpoint function of *MRC1*37, had little effect on single copy sequence-mediated GCRs but caused a large increase in duplication-mediated GCRs (Table 3). Similarly, deleting *TOF1*, which encodes another replication fork and checkpoint protein39, caused a specific increase in *HXT13 DSF1* duplication-mediated GCRs (Table 3). We found a synergistic interaction between *mrc1*Δ and *tof1*Δ but not between *mrc1-aq* and *tof1*Δ in both the *yel068c::CAN1/URA3* and *yel072w::CAN1/URA3* assays, indicating a partial redundancy of these genes (Table 3).

Mutations in the checkpoint genes *RAD24*, *MEC1*, *RAD53*, *DUN1* and *CHK1* increased the GCR rate in both the *yel068c::CAN1/URA3* and *yel072w::CAN1/URA3* assays (Table 3), although the affect on duplication-mediated GCR rates was possibly not as large as that of *mrc1*Δ or *tof1*Δ mutations, raising the possibility that *mrc1*Δ and *tof1*Δ mutations might increase DNA damage in addition to causing checkpoint defects. Mutations in *TEL1*, which encodes a protein kinase that is partially redundant with Mec1, resulted in small rate increases in both GCR assays, consistent with a small checkpoint role for Tel1 in the presence of Mec1; however, *tel1*Δ telomere maintenance defects could contribute to a low level of GCRs. Mutations in *RAD9*, which encodes an alternative Rad53 co-activator that responds to general DNA damage signaling, but not replication fork damage in strains with *MRC1*39, were similar to the affects of damage checkpoint mutations on single copy sequence-mediated GCRs, but caused a much smaller increase than these mutations in the rate of duplication-mediated GCRs. Together, these data suggest that the DNA damage checkpoint primarily suppresses single copy sequence-mediated GCRs whereas both the DNA damage checkpoint to a lesser extent and the replication stress checkpoint to a much greater extent suppress duplication-mediated GCRs.

DISCUSSION

We have found that many genes play little or no role in suppressing GCRs in single-copy sequences but play a large role in suppressing GCRs mediated by non-allelic HR at the *HXT13 DSF1* “at risk” sequence that resembles a segmental duplication in mammalian cells. One group of genes include the MMR genes and the genes encoding the Sgs1-Top3-Rmi1 complex that suppress HR between divergent sequences29. Another group included *MRC1* and *TOF1*, and our analysis of checkpoint genes indicated that the replication stress checkpoint is critical in suppressing *HXT13 DSF1* mediated GCRs but not single-copy sequence mediated GCRs. A third group of genes that almost all exclusively function in

suppressing *HXT13 DSF1* duplication-mediated GCRs include *SRS2*, *RRM3*, *MUS81*, *SLX1*, *SLX2*, *SLX4*, *SLX5*, and *SLX8*, which cause synthetic growth defects when deleted in combination with an *sgs1*Δ mutation, due to accumulation of toxic replication intermediates that in many cases can be suppressed by a HR defect40-43. Potentially related to these genes are: *RAD10* and *EXO1* that encode an endonuclease and an exonuclease, respectively, that can act in processing of HR and aberrant replication intermediates44, 45; *MPH1* encoding a DNA helicase that may disrupt HR intermediates like Sgs146-48; and *RAD6* that regulates processes that act on replication forks that encounter DNA damage49. Finally, *ARP8*, *NHP10*, *ASF1* and *RTT109*, which function in chromatin remodeling and checkpoint regulation and can act during S-phase35, 50, strongly suppressed duplication-mediated GCRs. All of these genes may function in responses to replication stress, including checkpoint activation or shut-off, repair of aberrant replication intermediates and suppression of the formation of aberrant replication intermediates, and some clearly act to directly prevent aberrant HR. How might the products of these genes act so specifically to prevent duplication mediated GCRs? It is unlikely that they solely act to prevent aberrant DNA structures during replication such as DSBs as they would also suppress GCRs mediated by single copy DNA sequences. Rather, they may prevent aberrant HR such as homeologous recombination or aberrant BIR intermediates so that HR can selectively target homologous sequences on sister chromatids and homologs as well as restart damaged replication forks to prevent genome instability rather than result in HR-mediated GCRs.

Our results indicate that dispersed repetitive elements in DNA resembling segmental duplications are “at-risk” for causing genomic instability. The presence of multiple pathways that are highly specific for suppressing rearrangements between these elements explains how genomes remain stable despite the presence of sequences “at risk” for mediating genome rearrangements. These results complement previous studies that identified critical pathways and genes that suppress GCRs that target single copy sequences17. Overall our data suggest that defects in different DNA repair pathways result in distinct GCR signatures that may be diagnostic of the defects that underlie genome instability.

METHODS SUMMARY

Yeast strains were constructed by deleting *CAN1* and integrating a telomeric hygromycin marker and a *CAN1/URA3* cassette in the RDKY3023 background (*MATa leu2*Δ*1 his3*Δ*200 trp1*Δ*63 lys2*Δ*Bgl hom3-10 ade2*Δ*1 ade8 ura3-52*). GCRs were selected using standard methods16. GCR products were analyzed by PCR and by aCGH (NimbleGen).

FULL METHODS

Plasmid construction

A *can1*::*hisG-URA3-hisG* disruption cassette was constructed by first PCR amplifying fragments that are telomeric to *CAN1* (Chr V 30187-30928) flanked by *Apa* I and *Xho* I sites and centromeric to *CAN1* (Chr V 34339-34965) flanked by *Xba* I and *Bam* HI sites and inserting them into pRS31551 to generate pRDK1374. A *hisG-URA3-hisG* fragment was amplified from pNKY5152 and was then inserted into *Sma* I-digested pRS315 by

recombinational cloning in *S. cerevisiae*. Then the *hisG-URA3-hisG* fragment was then subcloned into pRDK1374 between *Sal* I and *Bam* HI sites to generate pRDK1375 containing the *hisG-URA3-hisG* fragment flanked by 626 bp of upstream and 741 bp of downstream homology to the *CAN1* locus.

The *CAN1/URA3* cassette was constructed by cloning fragments of *CAN1* and *URA3* into a plasmid with flanking *Nhe* I sites. The *CAN1* gene and flanking sequence (Chr V 30952-34315) was amplified by PCR and cloned into pCR2.1-TOPO (Invitrogen) to generate pRDK1376. The *URA3* gene and flanking sequence (Chr V 116011- 117061) was amplified by PCR with primers to introduce flanking *Xba* I sites, and cloned into pRDK1376; inserts with *CAN1* and *URA3* in divergent orientations were selected. The *CAN1/URA3* cassette was then PCR amplified with primers adding flanking *Nhe* I sites, cloned into pCRT7CT (Invitrogen), and verified by sequencing to generate pRDK1377.

For each chromosome V integration site, integration constructs were generated by subcloning the pRDK1377 *Nhe* I fragment into plasmids containing the target genes of interest. The gene and flanking regions of *YEL072W* (Chr V 12961-14898) and *YEL068C* (Chr V 25222-26411) were amplified by PCR, cloned into pRS315, and modified by site-directed mutagenesis to introduce *Nhe* I sites into the center of the genes. Subcloning the *CAN1/URA3* cassette into the engineered *Nhe* I sites in *YEL072W* and *YEL068C* generated the plasmids pRDK1378 and pRDK1379, respectively. Similarly, the gene and flanking regions of *YEL064C* (Chr V 30060-30928) and *YEL062W* (Chr V 36007-36992) were amplified by PCR, cloned into pET21a, and the *Nhe* I-digested *CAN1/URA3* cassette was subcloned into compatible *Spe* I sites to generate plasmids pRDK1380 and pRDK1381, respectively.

Genetic Methods

YPD and synthetic drop-out media for propagation of strains have been described previously53. The *can1::hisG-URA3-hisG* integration fragment was cut out from pRDK1375 using *Kpn* I and *Sac* I and transformed into RDKY3023 (MATa leu2Δ1 his3Δ200 trp1Δ63 lys2ΔBgl hom3-10 ade2Δ1 ade8 ura3-52). Uracil prototrophs were verified by PCR, and a *can1::hisG* uracil auxotroph, RDKY5461, was selected on 5FOA containing medium. The *CAN1/URA3* integration cassettes were amplified by PCR from plasmids described above and integrated into RDKY5461. These strains were then modified by integrating a hygromycin resistance cassette telomeric to *YEL072W* (Chr V 11081-11618) to generate RDKY6678 (*yel072w::CAN1/URA3*), RDKY6677 (*yel068c::CAN1/URA3*), RDKY6676 (*yel064c::CAN1/URA3*), and RDKY6675 (*yel062w::CAN1/URA3*). Additional mutations were added to these strains using standard PCR-based mutagenesis methods, pop-in, pop-out plasmid vectors or intercrossing with mutants derived from the same parental strain background (Supplemental Table 2). The media and protocol for measuring GCR rates were essentially as described previously53. 95% confidence intervals of the median were calculated by the a two-sided nonparametric test (http://www.math.unb.ca/~knight/utility/MedInt95.htm). The GCR rates determined using this method are highly reliable. Using data from a number of studies covering a broad range of mutants and GCR rates, we have calculated that the average upper and ower 95%

confidence interval limits are 1.5 and 0.7, respectively, times the median GCR rate determined. In less than 8% of the measurements were the upper and lower 95% confidence intervals greather than 2 or less than 0.5, respectively, times the median GCR rate determined.

Analysis of GCR Isolates

GCR isolates were tested for loss of hygromycin resistance by growth on YPD media containing 300 μg/mL hygromycin B (Invitrogen). Genomic DNA was prepared from individual isolates and subjected to PCR analysis to categorize GCRs. The t(V;XIV) and t(V;IV or X) translocations were identified by amplification of the junction region with a Chr V-specific primer centromeric to the *HXT13 DSF1* region and a Chr XIV or Chr IV/X specific primer telomeric to the *HXT13 DSF1* homologies on those chromosomes under conditions where no product was generated with DNA from wild-type strains. A series of PCR reactions spanning the ~20 kb region between HXT13 and PCM1 on Chr V were used to map breakpoints for isolates that were not t(V;XIV) or t(V;IV or X) translocations by identifying the region where all telomeric reactions failed and all centromeric reactions succeeded. Breakpoint junctions from selected t(V;XIV) isolates were amplified as described above and sequenced by dye terminator DNA sequencing.

Array Comparative Genomic Hybridization

1 ug of genomic DNA was prepared from GCR isolates and wild-type RDKY6678 using the Purgene kit (Qiagen) and concentrated to over 100 ng/uL. GCR isolate DNA was amplified and labeled with Cy5 and the wild-type DNA was amplified and labeled with Cy3 and GCR isolate/wild-type pairs were applied to a NimbleGen 4-plex chip. Data were analyzed using the SignalMap software (NimbleGen).

Supplementary Material

Refer to Web version on PubMed Central for supplementary material.

ACKNOWLEDGEMENTS

We thank the UCSD Microarray Core Facility for assistance in the aCGH experiments and Cathy Smith, Scarlet Shell, and John Petrini for helpful comments on the manuscript. This work was supported by NIH grant GM26017.

REFERENCES

1. OMIM. (Institute of Genetic Medicine, Johns Hopkins University (Baltimore MD) and National Center for Biotechnology Information, National Library of Medicine, 1999)
2. Stankiewicz P, Lupski JR. The genomic basis of disease, mechanisms and assays for genomic disorders. Genome Dyn. 2006; 1:1–16. [PubMed: 18724050]
3. Mitelman, F. Catalog of chromosome aberrations in cancer. Wiley Liss; New York, N. Y.: 1991.
4. Gorringe KL, et al. Evidence that both genetic instability and selection contribute to the accumulation of chromosome alterations in cancer. Carcinogenesis. 2005; 26:923–30. [PubMed: 15677628]
5. Lengauer C, Kinzler KW, Vogelstein B. Genetic instability in colorectal cancers. Nature. 1997; 386:623–7. [PubMed: 9121588]

6. Ribas M, et al. The structural nature of chromosomal instability in colon cancer cells. Faseb J. 2003; 17:289–91. [PubMed: 12475895]
7. Hoeijmakers JH. Genome maintenance mechanisms for preventing cancer. Nature. 2001; 411:366–74. [PubMed: 11357144]
8. Deininger PL, Batzer MA. Alu repeats and human disease. Mol Genet Metab. 1999; 67:183–93. [PubMed: 10381326]
9. Gordenin DA, Resnick MA. Yeast ARMs (DNA at-risk motifs) can reveal sources of genome instability. Mutat Res. 1998; 400:45–58. [PubMed: 9685581]
10. Batzer MA, Deininger PL. Alu repeats and human genomic diversity. Nat Rev Genet. 2002; 3:370–9. [PubMed: 11988762]
11. Ji Y, Eichler EE, Schwartz S, Nicholls RD. Structure of chromosomal duplicons and their role in mediating human genomic disorders. Genome Res. 2000; 10:597–610. [PubMed: 10810082]
12. Harris S, Rudnicki KS, Haber JE. Gene conversions and crossing over during homologous and homeologous ectopic recombination in Saccharomyces cerevisiae. Genetics. 1993; 135:5–16. [PubMed: 8224827]
13. Umezu K, Hiraoka M, Mori M, Maki H. Structural analysis of aberrant chromosomes that occur spontaneously in diploid Saccharomyces cerevisiae: retrotransposon Ty1 plays a crucial role in chromosomal rearrangements. Genetics. 2002; 160:97–110. [PubMed: 11805048]
14. Lemoine FJ, Degtyareva NP, Lobachev K, Petes TD. Chromosomal translocations in yeast induced by low levels of DNA polymerase a model for chromosome fragile sites. Cell. 2005; 120:587–98. [PubMed: 15766523]
15. Lobachev KS, et al. Inverted Alu repeats unstable in yeast are excluded from the human genome. Embo J. 2000; 19:3822–30. [PubMed: 10899135]
16. Chen C, Kolodner RD. Gross chromosomal rearrangements in Saccharomyces cerevisiae replication and recombination defective mutants. Nat Genet. 1999; 23:81–5. [PubMed: 10471504]
17. Putnam CD, Pennaneach V, Kolodner RD. Saccharomyces cerevisiae as a model system to define the chromosomal instability phenotype. Mol Cell Biol. 2005; 25:7226–38. [PubMed: 16055731]
18. Eichler EE. Recent duplication, domain accretion and the dynamic mutation of the human genome. Trends Genet. 2001; 17:661–9. [PubMed: 11672867]
19. Bosco G, Haber JE. Chromosome break-induced DNA replication leads to nonreciprocal translocations and telomere capture. Genetics. 1998; 150:1037–47. [PubMed: 9799256]
20. Deem A, et al. Defective break-induced replication leads to half-crossovers in Saccharomyces cerevisiae. Genetics. 2008; 179:1845–60. [PubMed: 18689895]
21. Boulton SJ, Jackson SP. Components of the Ku-dependent non-homologous end-joining pathway are involved in telomeric length maintenance and telomeric silencing. Embo J. 1998; 17:1819–28. [PubMed: 9501103]
22. Smith CE, Llorente B, Symington LS. Template switching during break-induced replication. Nature. 2007; 447:102–5. [PubMed: 17410126]
23. Schmidt KH, Wu J, Kolodner RD. Control of translocations between highly diverged genes by Sgs1, the Saccharomyces cerevisiae homolog of the Bloom's syndrome protein. Mol Cell Biol. 2006; 26:5406–20. [PubMed: 16809776]
24. Oh SD, et al. BLM ortholog, Sgs1, prevents aberrant crossing-over by suppressing formation of multichromatid joint molecules. Cell. 2007; 130:259–72. [PubMed: 17662941]
25. Myung K, Chen C, Kolodner RD. Multiple pathways cooperate in the suppression of genome instability in Saccharomyces cerevisiae. Nature. 2001; 411:1073–6. [PubMed: 11429610]
26. Krogh BO, Symington LS. Recombination proteins in yeast. Annu Rev Genet. 2004; 38:233–71. [PubMed: 15568977]
27. Bai Y, Symington LS. A Rad52 homolog is required for RAD51-independent mitotic recombination in Saccharomyces cerevisiae. Genes Dev. 1996; 10:2025–37. [PubMed: 8769646]
28. Datta A, Adjiri A, New L, Crouse GF, Jinks Robertson S. Mitotic crossovers between diverged sequences are regulated by mismatch repair proteins in Saccaromyces cerevisiae. Mol Cell Biol. 1996; 16:1085–93. [PubMed: 8622653]

29. Myung K, Datta A, Chen C, Kolodner RD. SGS1, the Saccharomyces cerevisiae homologue of BLM and WRN, suppresses genome instability and homeologous recombination. Nat Genet. 2001; 27:113–6. [PubMed: 11138010]
30. Sugawara N, Goldfarb T, Studamire B, Alani E, Haber JE. Heteroduplex rejection during single-strand annealing requires Sgs1 helicase and mismatch repair proteins Msh2 and Msh6 but not Pms1. Proc Natl Acad Sci U S A. 2004; 101:9315–20. [PubMed: 15199178]
31. Mullen JR, Nallaseth FS, Lan YQ, Slagle CE, Brill SJ. Yeast Rmi1/Nce4 controls genome stability as a subunit of the Sgs1-Top3 complex. Mol Cell Biol. 2005; 25:4476–87. [PubMed: 15899853]
32. Lydeard JR, Jain S, Yamaguchi M, Haber JE. Break-induced replication and telomerase-independent telomere maintenance require Pol32. Nature. 2007; 448:820–3. [PubMed: 17671506]
33. Zou H, Rothstein R. Holliday junctions accumulate in replication mutants via a RecA homolog-independent mechanism. Cell. 1997; 90:87–96. [PubMed: 9230305]
34. Hwang JY, Smith S, Myung K. The Rad1-Rad10 complex promotes the production of gross chromosomal rearrangements from spontaneous DNA damage in Saccharomyces cerevisiae. Genetics. 2005; 169:1927–37. [PubMed: 15687264]
35. Conaway RC, Conaway JW. The INO80 chromatin remodeling complex in transcription, replication and repair. Trends Biochem Sci. 2009; 34:71–7. [PubMed: 19062292]
36. Mayer ML, Gygi SP, Aebersold R, Hieter P. Identification of RFC(Ctf18p, Ctf8p, Dcc1p): an alternative RFC complex required for sister chromatid cohesion in S. cerevisiae. Mol Cell. 2001; 7:959–70. [PubMed: 11389843]
37. Osborn AJ, Elledge SJ. Mrc1 is a replication fork component whose phosphorylation in response to DNA replication stress activates Rad53. Genes Dev. 2003; 17:1755–67. [PubMed: 12865299]
38. Roberts TM, Zaidi IW, Vaisica JA, Peter M, Brown GW. Regulation of rtt107 recruitment to stalled DNA replication forks by the cullin rtt101 and the rtt109 acetyltransferase. Mol Biol Cell. 2008; 19:171–80. [PubMed: 17978089]
39. Katou Y, et al. S-phase checkpoint proteins Tof1 and Mrc1 form a stable replication-pausing complex. Nature. 2003; 424:1078–83. [PubMed: 12944972]
40. Mullen JR, Kaliraman V, Ibrahim SS, Brill SJ. Requirement for three novel protein complexes in the absence of the Sgs1 DNA helicase in Saccharomyces cerevisiae. Genetics. 2001; 157:103–18. [PubMed: 11139495]
41. Schmidt KH, Kolodner RD. Requirement of Rrm3 helicase for repair of spontaneous DNA lesions in cells lacking Srs2 or Sgs1 helicase. Mol Cell Biol. 2004; 24:3213–26. [PubMed: 15060145]
42. Fabre F, Chan A, Heyer WD, Gangloff S. Alternate pathways involving Sgs1/Top3, Mus81/Mms4, and Srs2 prevent formation of toxic recombination intermediates from single-stranded gaps created by DNA replication. Proc Natl Acad Sci U S A. 2002; 99:16887–92. [PubMed: 12475932]
43. Torres JZ, Schnakenberg SL, Zakian VA. Saccharomyces cerevisiae Rrm3p DNA helicase promotes genome integrity by preventing replication fork stalling: viability of rrm3 cells requires the intra-S-phase checkpoint and fork restart activities. Mol Cell Biol. 2004; 24:3198–212. [PubMed: 15060144]
44. Sugawara N, Paques F, Colaiacovo M, Haber JE. Role of Saccharomyces cerevisiae Msh2 and Msh3 repair proteins in double-strand break-induced recombination. Proc Natl Acad Sci U S A. 1997; 94:9214–9. [PubMed: 9256462]
45. Fiorentini P, Huang KN, Tishkoff DX, Kolodner RD, Symington LS. Exonuclease I of Saccharomyces cerevisiae functions in mitotic recombination in vivo and in vitro. Mol Cell Biol. 1997; 17:2764–73. [PubMed: 9111347]
46. Krejci L, et al. DNA helicase Srs2 disrupts the Rad51 presynaptic filament. Nature. 2003; 423:305–9. [PubMed: 12748644]
47. Prakash R, et al. Yeast Mph1 helicase dissociates Rad51-made D-loops: implications for crossover control in mitotic recombination. Genes Dev. 2009; 23:67–79. [PubMed: 19136626]
48. Veaute X, et al. The Srs2 helicase prevents recombination by disrupting Rad51 nucleoprotein filaments. Nature. 2003; 423:309–12. [PubMed: 12748645]
49. Hoege C, Pfander B, Moldovan GL, Pyrowolakis G, Jentsch S. RAD6-dependent DNA repair is linked to modification of PCNA by ubiquitin and SUMO. Nature. 2002; 419:135–41. [PubMed: 12226657]

50. Chen CC, et al. Acetylated lysine 56 on histone H3 drives chromatin assembly after repair and signals for the completion of repair. Cell. 2008; 134:231–43. [PubMed: 18662539]

51. Sikorski RS, Hieter P. A system of shuttle vectors and yeast host strains designed for efficient manipulation of DNA in *Saccharomyces cerevisiae*. Genetics. 1989; 122:19–27. [PubMed: 2659436]

52. Alani E, Cao L, Kleckner N. A method for gene disruption that allows repeated use of *URA3* selection in the construction of multiply disrupted yeast strains. Genetics. 1987; 116:541–5. [PubMed: 3305158]

53. Chen C, Kolodner RD. Gross chromosomal rearrangements in *Saccharomyces cerevisiae* replication and recombination defective mutants. Nat Genet. 1999; 23:81–5. [PubMed: 10471504]

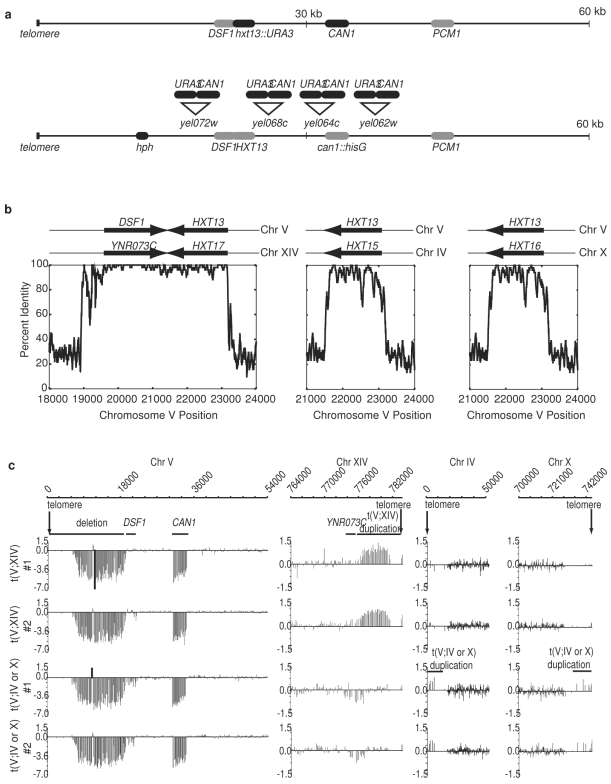

Figure 1. New assays for evaluating the genes that suppress the accumulation of GCRs

A. The standard chromosome V GCR assay (top) contains *URA3* integrated at *HXT13* and selects for GCRs with Chr V breakpoints located between *CAN1* and the essential *PCM1* gene. The modified GCR assays (bottom) have a *CAN1/URA3* cassette inserted into *YEL062W*, *YEL064C*, *YEL068C*, and *YEL072W* in a strain with *ura3-52* and *can1*∷*hisG* mutations and a telomeric hygromycin resistance marker (*hph*). **B**. The average percent identity in 50 bp windows with the *HXT13 DSF1* region with regions of chromosomes XIV, X, and IV is plotted against the Chr V position. **C**. aCGH data ($\log_2$ of the fluorescence ratio of individual GCR isolates to wild-type) indicates that the region from the Chr V homologies to the target chromosome telomere was duplicated. The two t(V;XIV) fusions lost unique Chr V signals telomeric to the *HXT13 DSF1* region (Chr V 1-19500) and *CAN1* from the *CAN1/URA3* cassette (ChrV 31694-33466). Increased signals were observed with all probes for Chr XIV telomeric to *YNR073C* (Chr XIV 776300-787000). The two t(V;IV or X) fusions had Chr V signals similar to the t(V;XIV) fusions and essentially unchanged Chr XIV signals, excepting a subtle loss of signal in the *DSF1* and *YNR073C* regions (Chr V 19589-21097; Chr XIV 774792-776300), consistent with loss of cross hybridization of *DSF1* DNA to probes for *DSF1*-like genes. Increased fluorescence of the left arm of Chr IV and the right arm of Chr X demonstrated amplification and cross hybridization between these almost identical regions, despite the scarcity of probes. The aCGH data revealed no other significant copy number changes, excepting the region indicating loss of *URA3* from the *CAN1/URA3* cassette (data not shown).

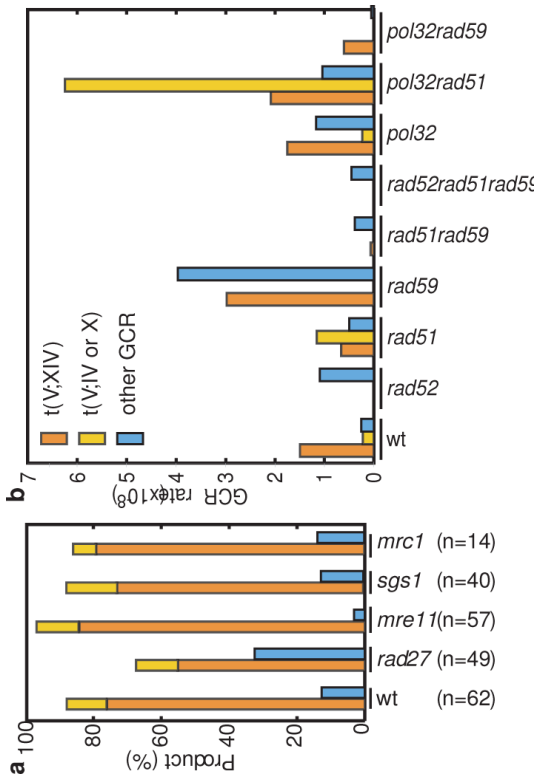

Figure 2. Summary of the types of GCRs detected in the *HXT13 DSF1* region mediated GCR assay

A. Percentage of the different types of GCRs in wild-type, *rad27*Δ, *mre11*Δ, *sgs1*Δ, and *mrc1*Δ *yel072*::*CAN1/URA3* strains. The homology-driven GCRs are shown as a stacked bar with t(V;XIV) in orange and t(V;IV or X) in yellow, and single-copy sequence mediated GCRs in blue. **B**. Mutations affecting both HR and BIR alter the rates of the formation of t(V;XIV), t(V;IV or X) and other GCRs detected in the *yel072*::*CAN1/URA3* assay. Rates for each class of GCR were calculated by multiplying the fraction of each kind of rearrangement by the overall rate.

Table 1

GCR rates for different positions of the *CAN1/URA3* cassette on chromosome V.

Assay	Wild-type		rad27Δ		mre11Δ		sgs1Δ		Breakpoint Region Length (kb)**	Wild-type Rate / Length (kb^{-1})
	Strain RDKY#	Rate*	Strain RDKY#	Rate*	Strain RDKY#	Rate*	Strain RDKY#	Rate*		
Standard GCR***	3615	3.5×10^{-10} (1)	3630	3.7×10^{-7} (1057)	3633	2.2×10^{-7} (629)	3813	2.5×10^{-8} (71)	11.6	3.0×10^{-11}
yel062w::CAN1/URA3	6675	1.15 [0.0-5.6]$\times10^{-10}$ (0.3)	6679	6.87×10^{-7} (2180)	6680	3.23×10^{-7} (496)	6681	1.19×10^{-8} (34)	9.7	1.2 [0.0-5.7]$\times10^{-11}$
yel064c::CAN1/URA3	6676	5.09 [2.5-7.7]$\times10^{-10}$ (1.6)	6682	7.47×10^{-7} (2371)	6683	2.63×10^{-7} (465)	6684	1.77×10^{-8} (51)	14.5	3.5 [1.7-5.3]$\times10^{-11}$
yel068c::CAN1/URA3	6677	2.27 [1.3-4.8]$\times10^{-9}$ (7.2)	6685	5.57×10^{-7} (1591)	6686	5.75×10^{-7} (1643)	6687	1.69×10^{-8} (48)	19.2	12 [6.8-25]$\times10^{-11}$
yel072::CAN1/URA3	6678	1.97 [1.6-4.3]$\times10^{-8}$ (56)	6688	2.78×10^{-6} (7943)	6689	1.52×10^{-6} (4345)	6690	1.93×10^{-6} (5515)	31.0	64 [52-140]$\times10^{-11}$
*yel068c::CAN1/URA3 hxt13-dsf1*Δ	6872	1.43 [0.0-4.2]$\times10^{-9}$ (4.1)	6873	3.74×10^{-7} (1068)	-	n.d.	6874	4.39×10^{-9} (12)	19.2	7.5 [0.0-22]$\times10^{-11}$
*yel072::CAN1/URA3 hxt13-dsf1*Δ	6875	5.64 [4.1-12]$\times10^{-9}$ (16)	6876	5.22×10^{-7} (1492)	-	n.d.	6877	1.17×10^{-8} (33)	27.7	20 [15-42]$\times10^{-11}$

*Rate of accumulating Can^R $5FOA^R$progeny. The number in parentheses is the fold increase relative to the standard wild-type rate (3.5×10^{-10}; 16). Numbers in brackets are the 95% confidence interval limits.

**The breakpoint region is defined as the length between the telomeric end of *PCM1* and the telomeric end of *CAN1*.

***Rates previously published16, 29.

Table 2

Effect of homologous and homeologous recombination defective mutations on GCR rates

Genotype	yel068c::CAN1/URA3		yel072w::CAN1/URA3		Ratio**
	Strain	GCR Rate*	Strain	GCR Rate*	
Wild-type	RDKY6677	2.27×10^{-9} (5.1)	RDKY6678	1.97×10^{-8} (56)	8.7
rad52 Δ	RDKY6691	1.67×10^{-8} (48)	RDKY6708	1.09×10^{-8} (31)	0.7
rad51 Δ	RDKY6692	$<2.63\times10^{-10}$ (<0.8)	RDKY6709	2.31×10^{-8} (66)	>88
rad59 Δ	RDKY6693	5.85×10^{-9} (17)	RDKY6710	6.94×10^{-8} (198)	11.9
*rad51*Δ *rad59*Δ	RDKY6694	2.92×10^{-9} (8.3)	RDKY6711	4.48×10^{-9} (13)	1.5
*rad51*Δ *rad59*Δ *rad52*Δ	RDKY6695	3.84×10^{-9} (11)	RDKY6712	4.53×10^{-9} (13)	1.2
msh2 Δ	RDKY6696	1.10×10^{-9} (3.1)	RDKY6713	1.75×10^{-7} (499)	159
msh6 Δ	RDKY6697	1.52×10^{-9} (4.4)	RDKY6714	2.10×10^{-7} (599)	138
msh3 Δ	RDKY6698	1.42×10^{-9} (4.1)	RDKY6715	3.67×10^{-8} (105)	26
mlhl Δ	RDKY6699	5.80×10^{-10} (1.7)	RDKY6716	3.85×10^{-8} (110)	66
sgsl Δ	RDKY6687	1.69×10^{-8} (48)	RDKY6690	1.93×10^{-6} (5515)	114
*sgs1*Δ *rad52*Δ	RDKY6700	7.75×10^{-8} (222)	RDKY6717	8.07×10^{-8} (231)	1.0
top3 Δ	RDKY6701	$<1.64\times10^{-9}$ (<4.7)	RDKY6718	2.14×10^{-6} (6103)	>1300
rmi1 Δ	RDKY6702	1.41×10^{-7} (404)	RDKY6719	1.27×10^{-5} (36700)	98.3
pol32 Δ	RDKY6703	3.41×10^{-9} (9.4)	RDKY6720	3.15×10^{-8} (90.0)	9.24
*pol32*Δ *rad51*Δ	RDKY6704	3.00×10^{-8} (86)	RDKY6721	9.37×10^{-8} (268)	3.1
*pol32*Δ *rad59*Δ	RDKY6705	5.50×10^{-10} (1.6)	RDKY6722	6.52×10^{-9} (19)	12
pri2-1 (23 deg)	RDKY6706	$<3.93\times10^{-10}$ (<1.1)	RDKY6723	7.10×10^{-10} (2.0)	>1.8
pol12-100 (23 deg)	RDKY6707	6.35×10^{-9} (18.1)	RDKY6724	2.31×10^{-8} (66.1)	3.7

*Rate of accumulating Can^R $5FOA^R$ progeny. The number in parentheses is the fold increase relative to the standard wildtype rate (3.5×10^{-10};16).

**The *yel072w::CAN1/URA3* rate divided by the *yel068c::CAN1/URA3* rate.

Table 3

Effect of mutations on the accumulation of duplication-mediated rearrangements

Genotype	yel068c::CAN1/URA3		yel072w::CAN1/URA3		Ratio**
	Strain	GCR Rate*	Strain	GCR Rate*	
Wild-type	RDKY6677	2.27×10^{-9} (5.1)	RDKY6678	1.97×10^{-8} (56)	8.7
***SGS1* interactors**					
mus81 Δ	RDKY6731	1.26×10^{-8} (36)	RDKY6748	2.51×10^{-7} (717)	20
rrm3 Δ	RDKY6735	9.46×10^{-10} (2.7)	RDKY6752	3.87×10^{-8} (110)	41
sae2 Δ	RDKY6737	$4.23\Delta10^{-8}$ (120)	RDKY6754	1.65×10^{-7} (470)	3.9
slx1 Δ	RDKY6738	$<1.12\times10^{-9}$ (<3.2)	RDKY6755	2.32×10^{-8} (66)	>20.6
slx4 Δ	RDKY6739	$<7.94\times10^{-10}$ (<2.3)	RDKY6756	9.26×10^{-8} (264)	>116
slx5 Δ	RDKY6740	1.48×10^{-9} (4.2)	RDKY6757	4.82×10^{-7} (1378)	326
slx8 Δ	RDKY6846	$<1.81\times10^{-9}$ (<5.2)	RDKY6847	9.65×10^{-7} (2757)	>532
srs2 Δ	RDKY6741	7.18×10^{-10} (2.1)	RDKY6758	1.28×10^{-7} (365)	178
Chromatin					
asf1 Δ	RDKY6725	1.34×10^{-8} (38)	RDKY6742	2.89×10^{-7} (825)	22
arp8 Δ	RDKY6726	$<6.05\times10^{-10}$ (<1.73)	RDKY6743	4.84×10^{-8} (138)	>80
nhp10 Δ	RDKY6732	1.39×10^{-9} (4.0)	RDKY6749	3.01×10^{-8} (86)	22
rtt109 Δ	RDKY6736	5.64×10^{-9} (16)	RDKY6753	1.84×10^{-7} (526)	33
Cohesion					
ctf18 Δ	RDKY6727	2.40×10^{-8} (69)	RDKY6744	2.22×10^{-7} (633)	9.2
Other Repair					
esc2 Δ	RDKY6878	4.36×10^{-8} (124)	RDKY6879	1.07×10^{-5} (30700)	247
esc4 Δ	RDKY6728	1.66×10^{-8} (48)	RDKY6745	3.07×10^{-7} (876)	18.5
exo1 Δ	RDKY6729	2.00×10^{-9} (5.7)	RDKY6746	8.44×10^{-8} (241)	42
mph1 Δ	RDKY6794	2.00×10^{-9} (5.7)	RDKY6795	1.05×10^{-7} (300)	53
rad6 Δ	RDKY6733	4.66×10^{-9} (13)	RDKY6750	6.03×10^{-7} (1724)	130
rad10 Δ	RDKY6734	8.49×10^{-10} (2.4)	RDKY6751	1.80×10^{-7} (404)	212

Genotype	yel068c::CAN1/URA3		yel072w::CAN1/URA3		Ratio**
	Strain	GCR Rate*	Strain	GCR Rate*	
Checkpoint					
mrc1 Δ	RDKY6730	3.35×10^{-9} (9.6)	RDKY6747	3.75×10^{-7} (1071)	112
mrc1-aq	RDKY6766	1.51×10^{-9} (4.3)	RDKY6775	1.23×10^{-7} (351)	81
tof1 Δ	RDKY6767	5.71×10^{-9} (16)	RDKY6776	4.25×10^{-7} (1214)	74
*mrc1*Δ *tof1*Δ	RDKY6779	6.41×10^{-8} (183)	RDKY6780	1.26×10^{-6} (3612)	20
mrc1-aq tof1 Δ	RDKY6848	3.69×10^{-9} (11)	RDKY6849	2.06×10^{-7} (589)	56
rad24 Δ	RDKY6759	2.00×10^{-8} (57.3)	RDKY6768	1.97×10^{-7} (555)	9.7
*mec1*Δ *sml1*Δ	RDKY6760	2.34×10^{-8} (67)	RDKY6769	1.50×10^{-7} (429)	6.4
tel1 Δ	RDKY6761	4.99×10^{-9} (14)	RDKY6770	2.87×10^{-8} (82)	5.8
*rad53*Δ *sml1*Δ	RDKY6762	5.60×10^{-8} (160)	RDKY6771	3.05×10^{-7} (871)	5.4
rad9 Δ	RDKY6765	2.17×10^{-8} (62)	RDKY6774	3.82×10^{-8} (109)	1.8
chk1 Δ	RDKY6764	1.76×10^{-8} (50)	RDKY6773	1.96×10^{-7} (560)	11
dun1 Δ	RDKY6763	1.63×10^{-8} (47)	RDKY6772	1.61×10^{-7} (461)	9.9

*Rate of accumulating Can^R $5FOA^R$progeny. The number in parentheses is the fold increase relative to the standard wildtype rate (3.5×10^{-10};16).

**The *yel072w::CAN1/URA3* rate divided by the *yel068c::CAN1/URA3* rate.